cmgh
CELLULAR AND MOLECULAR GASTROENTEROLOGY AND HEPATOLOGY

ORIGINAL RESEARCH

Dysregulated Intrahepatic CD4$^+$ T-Cell Activation Drives Liver Inflammation in Ileitis-Prone SAMP1/YitFc Mice

Sara Omenetti,[1,2] Marco Brogi,[1,2] Wendy A. Goodman,[1] Colleen M. Croniger,[3] Saada Eid,[4] Alex Y. Huang,[1,4] Giacomo Laffi,[2] Tania Roskams,[5] Fabio Cominelli,[1,2,6] Massimo Pinzani,[2,6,7,*] and Theresa T. Pizarro[1,2,6,*]

[1]Department of Pathology, Case Western Reserve University School of Medicine, Cleveland, Ohio; [2]"DENOThe" Center, University of Florence, Florence, Italy; [3]Department of Nutrition, Case Western Reserve University School of Medicine, Cleveland, Ohio; [4]Department of Pediatrics, Case Western Reserve University School of Medicine, Cleveland, Ohio; [5]Department of Morphology and Molecular Pathology, University of Leuven, Leuven, Belgium; [6]Department of Medicine, Case Western Reserve University School of Medicine, Cleveland, Ohio; [7]UCL Institute for Liver and Digestive Health, Royal Free Hospital, London, United Kingdom

SUMMARY

Ileitis-prone SAMP1/YitFc mice display concomitant immune-mediated liver inflammation, which is driven by hyperactivated intrahepatic T_H1 CD4$^+$ T effector cells. Locally impaired hepatic immunosuppression rather than recruitment of gut-derived cells is likely responsible for the heightened activation status of these cells.

BACKGROUND & AIMS: Liver inflammation is a common extraintestinal manifestation of inflammatory bowel disease (IBD), but whether liver involvement is a consequence of a primary intestinal defect or results from alternative pathogenic processes remains unclear. Therefore, we sought to determine the potential pathogenic mechanism(s) of concomitant liver inflammation in an established murine model of IBD.

METHODS: Liver inflammation and immune cell subsets were characterized in ileitis-prone SAMP1/YitFc (SAMP) and AKR/J (AKR) control mice, lymphocyte-depleted SAMP (SAMPx*Rag-1*$^{-/-}$), and immunodeficient SCID recipient mice receiving SAMP or AKR donor CD4$^+$ T cells. Proliferation and suppressive capacity of CD4$^+$ T-effector (Teff) and T-regulatory (Treg) cells from gut-associated lymphoid tissue (GALT) and livers of SAMP and AKR mice were measured.

RESULTS: Surprisingly, prominent inflammation was detected in 4-week-old SAMP livers before histologic evidence of ileitis, whereas both disease phenotypes were absent in age-matched AKR mice. SAMP liver disease was characterized by abundant infiltration of lymphocytes, required for hepatic inflammation to occur, a T_H1-skewed environment, and phenotypically activated CD4$^+$ T cells. SAMP intrahepatic CD4$^+$ T cells also had the ability to induce liver and ileal inflammation when adoptively transferred into SCID recipients, whereas GALT-derived CD4$^+$ T cells produced milder ileitis but not liver inflammation. Interestingly, SAMP intrahepatic CD4$^+$ Teff cells showed increased proliferation compared with both SAMP GALT- and AKR liver-derived CD4$^+$ Teff cells, and SAMP intrahepatic Tregs were decreased among CD4$^+$ T cells and impaired in in vitro suppressive function compared with AKR.

CONCLUSIONS: Activated intrahepatic CD4$^+$ T cells induce liver inflammation and contribute to experimental ileitis via locally impaired hepatic immunosuppressive function. *(Cell Mol Gastroenterol Hepatol 2015;1:406–419; http://dx.doi.org/10.1016/j.jcmgh.2015.05.007)*

Keywords: Hepatic CD4$^+$ T Cells; IBD-Associated Liver Inflammation; Liver Sinusoidal Endothelial Cells; Regulatory T Cells; SAMP1/YitFc Mice.

Liver disease constitutes one of the most frequently occurring extraintestinal manifestations of IBD, with primary sclerosing cholangitis (PSC) representing the most common hepatobiliary-associated ailment. Besides PSC, a wide range of liver pathologies have been reported in IBD patients, including PSC/autoimmune hepatitis (AIH) "overlap syndrome," IgG4-associated cholangitis, primary biliary cirrhosis, fatty liver, granulomatous hepatitis, cholelithiasis, and portal vein thrombosis.[1] Despite its prevalence, the precise etiology of liver inflammation during IBD is currently unknown.

To date, the most widely accepted hypothesis of IBD-associated liver disease, particularly PSC, is that it occurs as a consequence of aberrant adhesion molecule expression that promotes the recruitment of memory T cells, originally activated in the gut, to the liver where they drive hepatic

*Authors share senior authorship.

Abbreviations used in this paper: AIH, autoimmune hepatitis; AKR, AKR/J; ALP, alkaline phosphatase; ALT, alanine aminotransferase; APC, antigen-presenting cell; BM, bone marrow; BMC, bone marrow chimera; CCL25, CC chemokine ligand 25; DC, dendritic cell; FoxP3, forkhead box protein 3; FACS, fluorescence-activated cell sorting; GALT, gut-associated lymphoid tissue; IBD, inflammatory bowel disease; IFN, interferon; IL, interleukin; KC, Kupffer cell; LSEC, liver sinusoidal endothelial cell; MAdCAM-1, mucosal addressin cell adhesion molecule-1; MHC, major histocompatibility complex; MLN, mesenteric lymph node; NPLC, nonparenchymal liver cells; PSC, primary sclerosing cholangitis; SAMP, SAMP1/YitFc; SCID, severe combined immunodeficiency; Teff, effector T cell; Treg, regulatory T cell.

2352-345X
http://dx.doi.org/10.1016/j.jcmgh.2015.05.007

inflammation.[2] Specifically, expression of mucosal addressin cell adhesion molecule-1 (MAdCAM-1) and CC chemokine ligand 25 (CCL25), normally restricted to the intestinal endothelium and small bowel epithelium, respectively, and which comprise the conventional gut "postal code,"[3] have been implicated as key mediators in this process. In PSC, for example, MAdCAM-1 and CCL25 are aberrantly expressed by the portal and sinusoidal endothelium and suggest the importance of these homing molecules for the migration of T cells to the liver.[4,5] Together, these observations support the existence of an enterohepatic lymphocyte circulation that facilitates trafficking of T lymphocytes from the gut to the liver that can then promote liver inflammation.

Alternatively, emerging evidence suggests that T-lymphocyte priming can also occur locally in the liver during both homeostatic and pathologic conditions.[6–8] Liver-resident antigen-presenting cells (APC), such as liver sinusoidal endothelial cells (LSEC), dendritic cells (DC), and Kupffer cells (KC), are capable of interacting with naïve T cells and have the ability to induce regulatory T cell (Treg) differentiation and function,[9,10] thereby promoting hepatic immune tolerance.

Of the many available models of IBD, only few allow investigation of the earliest events associated with the onset and natural course of disease. SAMP1/YitFc (SAMP) mice represent a well-characterized model of spontaneous, chronic intestinal inflammation, whose primary disease location (ie, the terminal ileum), histologic features, and response to standard therapies closely resemble Crohn's disease, one of the idiopathic forms of IBD.[11,12] The SAMP strain was derived from several generations of brother-sister mating of parental AKR mice with ileitis but not colitis developing spontaneously without chemical, genetic, or immunologic manipulation.[11–13] Our initial findings of liver disease noted lymphocytic infiltration of hepatic portal tracts in 20- to 30-week-old SAMP mice,[13] previously reported by others;[14] however, this observation was never further characterized by either group. Accordingly, SAMP mice represent an ideal model to evaluate the onset and progression of liver inflammation in the presence of chronic ileitis and to investigate the relationship and potential mechanism(s) linking gut and liver pathologies.

Herein, we report both portal and lobular liver inflammation that occurs *before* the onset of gut inflammation in SAMP mice, an established mouse model of Crohn's disease-like ileitis. Further characterization of intrahepatic immune cells confirmed specific expansion of type 1 helper T (T_H1)-polarized $CD4^+$ T cells that drive severe liver as well as ileal inflammation when adoptively transferred into naïve SCID recipients. Importantly, intrahepatic $CD4^+$ T cells do not display a gut-tropic phenotype, suggesting that local over-activation rather than recruitment of gut-activated $CD4^+$ T cells may be responsible for the liver disease in SAMP. Indeed, impaired in vitro suppressive function of hepatic Tregs was observed in SAMP mice. Taken together, our results challenge the current paradigm that IBD-associated liver disease represents a secondary event to gut inflammation and raise the possibility that liver inflammation during IBD may develop as a consequence of impaired immune tolerance within the host liver, which may also influence the course of chronic intestinal inflammation in individuals predisposed to IBD.

Materials and Methods

Mice

Original AKR/J (AKR), B6.129S7-Rag1^{tm1Mom}/J (*Rag-1*$^{-/-}$), and C3Smn.CB17-Prkdcscid/J (SCID) mice were purchased from the Jackson Laboratory (Bar Harbor, ME). SAMP founders were originally provided by S. Matsumoto (Yakult Central Institute for Microbiological Research, Tokyo, Japan).[11,13] The SAMP*Rag-1*$^{-/-}$ strain was generated by backcrossing *Rag-1*$^{-/-}$ mice onto the SAMP background for 10 generations. All experimental mice were subsequently bred (>20 generations) and maintained under specific pathogen-free conditions, fed standard laboratory chow (Harlan Teklad, Indianapolis, IN), and kept on 12-hour light/dark cycles. All procedures followed Association for Assessment and Accreditation of Laboratory Animal Care guidelines and were approved by Case Western Reserve University's institutional animal care and use committee.

Liver Enzyme Levels

Sera from experimental mice were assayed 1:5 for alkaline phosphatase (ALP) (BioVision, Mountain View, CA), and undiluted for alanine aminotransferase (ALT) (Genzyme Diagnostics P.E.I., Charlottetown, PE, Canada) according to manufacturer's instructions.

Histology and Immunohistochemistry

Liver and ileal tissues were processed for histology[11,14–20] and evaluated by trained pathologists (T. Roskams, J. Mize) using a novel liver (Table 1) and an established ileal[14,16–22] scoring system. Immunolocalization of T cells was performed using αCD3 (ab5690/1:50) primary antibodies (Abcam, Cambridge, MA), and visualized using the Dako EnVision System (Dako, Carpinteria, CA). Images were obtained on an Axiophot microscope and assembled by Axiovision Release 4.5 (Carl Zeiss, Thornwood, NY).

Nonparenchymal Liver Cell Isolation

Nonparenchymal liver cells (NPLCs) were isolated by perfusing mice with Hank's balanced salt solution through the hepatic portal vein, after which livers were removed and homogenized. Homogenates were incubated with agitation at 37°C for 30 minutes in a solution of collagenase type IV and DNase I in Hank's balanced salt solution (Sigma-Aldrich, St. Louis, MO). Resulting cell suspensions were centrifuged at 300 rpm at 4°C, passed through μm nylon filters, and centrifuged again at 1200 rpm at 4°C for 10 minutes. ACK Lysing Buffer (Invitrogen, Carlsbad, CA) was added to cell pellets for 5 minutes at room temperature and similarly centrifuged. Cells were washed twice and used for immediate experimentation, or either further purified by centrifugation at 2500 rpm for 30 minutes through a 40%/70% Percoll gradient (Sigma-Aldrich) or enriched for $CD4^+$ T cells (described herein), after which the cells were washed twice and then used for experiments.

Table 1. Histologic Scoring System for Liver Disease in SAMP Mice

Area	Index	Grade	Description
Portal area	Portal	0	Normal
		1	Moderate portal tract expansion with lymphocytic infiltration
		2	As in 1, plus focal lymphocyte infiltration of the limiting plate
		3	Severe portal tract expansion with lymphocytic infiltration
		4	As in 3, plus piecemeal necrosis and periportal lymphocytic infiltration of the liver lobules
	Biliary	0	Normal
		1	Moderate lymphocytic infiltration around biliary ducts
		2	As in 1, plus focal lymphocyte infiltration of biliary epithelium
		3	Severe lymphocyte infiltration around biliary ducts
		4	Extensive biliary involvement with severe lymphocyte infiltration
Lobular area	Lobular	0	Normal
		1	Few lymphocytes scattered or clustered within lobular area
		2	Occasional granulomas
		3	Granulomas present in several lobular areas
		4	Large and/or confluent granulomas in all lobular areas
	Steatosis	0	Normal
		1	Moderate steatosis limited to controlobular area
		2	Moderate steatosis in all lobular areas
		3	Severe steatosis primarily in centrolobular area
		4	Massive, diffuse steatosis affecting all lobular areas

Note: Total liver inflammatory index is calculated by the sum of portal, biliary, lobular, and steatosis indices multiplied by the percentage of involvement, assigned as 1 = 0–25%, 2 = 26%–50%, 3 = 51%–75%, and 4 = 76%–100%.

Flow Cytometry

Single-cell suspensions were prepared from mesenteric lymph nodes (MLN)[18] and livers, and 10^6 cells stained with the following antibodies: fluorescein isothiocyanate-labeled CD8a (53–6.7), PerCP-labeled CD4 (RM4–5), APC-labeled CD25 (PC61), PE-labeled CD44 (IM7), (BD Pharmingen, San Diego, CA), APC-labeled $\alpha4\beta7$ (PS/2) (AbD Serotec, United Kingdom), PE-labeled CCR9 (242503) (R&D System, Minneapolis, MN), APC-labeled CD146 (ME-9F1), APC-Cy7 CD11c (N418), PE-labeled I-A^k (10–3.6), CD69 (H1.2F3), PE-Cy5 CD3 (145–2C11), fluorescein isothiocyanate-CD19 (6D5) (Biolegend, San Diego, CA), and eFluor 450-labeled F4/80 (BM8) (eBioscience, San Diego, CA). For intracellular staining, cells were fixed after cell-surface staining, followed by permeabilization and staining with PE-labeled forkhead box protein 3 (FoxP3) (FJK-16s) as per the manufacturer's instructions (eBioscience). Samples were analyzed with a FACSCalibur or LSR II and CellQuest Software (Becton Dickinson, San Jose, CA).

Adoptive Transfer Model

Livers and MLNs were harvested from 10- to 12-week-old donors, rendered into single-cell suspensions, and purified for $CD4^+$ lymphocytes using magnetic bead separation (Miltenyi Biotec, Auburn, CA). $CD4^+$ T cells (400,000) were transferred intraperitoneally into 6- to 8-week-old major histocompatibility complex (MHC)-matched SCIDs; untransferred SCIDs receiving phosphate-buffered saline (vehicle) served as controls. Six weeks after transfer, the recipient mice were euthanized, and the livers and ilea were processed for histologic evaluation and intrahepatic $CD4^+$ T-cell isolation, again using magnetic bead separation (Miltenyi Biotec).

Cytokine mRNA Expression

The NPLC and ex vivo-cultured αCD3/CD28-activated $CD4^+$ T cells[22] were lysed in Buffer RLT (Qiagen, Germantown, MD) immediately after collection. The total RNA was isolated using RNeasy Mini Kits (Qiagen) and reverse-transcribed to cDNA (RNA-to-cDNA kit; Applied Biosystems, Forest City, CA). Real-time quantitative polymerase chain reaction was performed using primers for T_H1 and T_H2 cytokines,[15] IL-33,[22] IL-1α (5′-TTTCCA CAGCCACGAAGCT-3′; 5′-TGATGAAAGGGCTCCCAAGTA-3′), IL-1β (5′-TCCTTAGTCCTCGGCCAAGAC-3′; 5′-GTGCCAT GGTTTCTTGTGACC-3′), and IL-18 (5′-CACTGTACAACCG CAGTAATACGG-3′; 5′-CAGCCAGTCCTCTTACTTCACTGT-3′), with target gene expression normalized to β-actin.

In Vitro T cell Functional Assays

The $CD4^+CD25^-$ effector T cells (Teff) and $CD4^+CD25^+$ (Treg) cells were isolated by fluorescence-activated cell sorting (FACS) from liver or MLN of SAMP and AKR mice. Teff cells were labeled with eFluor 670 (5-(6)-carboxyfluorescein diacetate succinimidyl ester analog, 0.5 μM) and cultured either with or without a 1:1 ratio of Tregs. $\alpha CD3^-$ (1 μg/mL), and $\alpha CD28^-$ (1 μg/mL) coated beads (Miltenyi Biotec) were added to cultures at a 1:0.8 Teff:bead ratio. Proliferation was determined after 3 days of culture by flow cytometric dye dilution assays.

MAdCAM-1 and CCL25 Protein Levels

Livers were collected and homogenized in radioimmunoprecipitation assay buffer supplemented with Halt proteases and phosphate inhibitor cocktail (Pierce Biotechnology, Rockford, IL), using lysing matrix tubes and FastPrep-24 (MP Biomedicals, Santa Ana, CA). Homogenates

were centrifuged at 12,000 rpm, the supernatants collected, and the total protein content measured using BCA Protein Assay kits (Pierce Biotechnology). After normalizing the protein content, we assayed the tissue homogenates for MAdCAM-1 and CCL25 protein by ELISA (R&D Systems).

Statistical Analysis

Two-tailed unpaired Student *t* test was performed using GraphPad Prism 5 (GraphPad Software, La Jolla, CA). The results are expressed as mean ± standard error of the mean (SEM); $P < .05$ was considered statistically significant. All authors had access to the study data and reviewed and approved the final manuscript.

Results

SAMP Mice Display Liver Inflammation Before the Onset of Ileitis

The onset of liver disease in SAMP mice was investigated because previous reports had described liver inflammation in 20- to 30-week-old adults[13,14] yet it was unknown whether younger mice also exhibited liver inflammation and when this phenotype initially emerged. Our results showed that elevated circulating levels of ALP and ALT were detected in 4-week-old SAMP mice compared with age-matched AKR mice (Figure 1*A*) when no histologic evidence of ileitis is generally present,[11–13] indicating that liver disease can precede ileitis. This was confirmed by histologic evaluation of SAMP livers that revealed diffuse inflammatory infiltrates involving both portal and lobular areas, even during the early stages of postnatal development at 1 week of age (see Figure 1*B* and *D*), which were absent in AKR livers (see Figure 1*C* and *E*). Conversely, adjacent intestinal tissues in both SAMP and AKR mice displayed completely normal morphology at this early age (see Figure 1*B* and *C*).

A detailed time-course study was then performed to further characterize the development of liver disease and coprogression with ileal inflammation. Histologic evaluation was done using a novel scoring system (see Table 1) on livers from SAMP and age/sex-matched AKR mice, based on critical time points in the development of SAMP ileitis, as follows: 3–4 weeks (before histologic evidence of ileitis, but presence of small intestinal epithelial permeability defect), 7–9 weeks (early, active phase of inflammation and dominant T_H1 cytokine profile), and >12 weeks (established, chronic inflammation and mixed T_H1/T_H2 cytokine profile); after 20 weeks, no significant differences are observed in the severity of ileitis among SAMP mice.[12]

A key observation in the present study was that peak liver inflammation occurred at 4 weeks in SAMP mice, when ileitis is normally absent (Figure 2*A*). Ileitis began to progressively increase in severity, reaching maximum inflammation by 20 weeks whereas liver inflammation gradually diminished, most significantly in areas of lobular compared with portal involvement (see Figure 2*A*). Consistent with these findings, at 20 weeks of age the circulating levels of ALP and ALT in SAMP mice were comparable to the AKR controls (Figure 3), indicative of the progressive decrease in the severity of liver inflammation. With regard to penetrance, the incidence of SAMP mice developing severe liver disease gradually decreased until 40 weeks (see Figure 2*B*); unlike in SAMP ileitis,[23] no sex differences were observed in

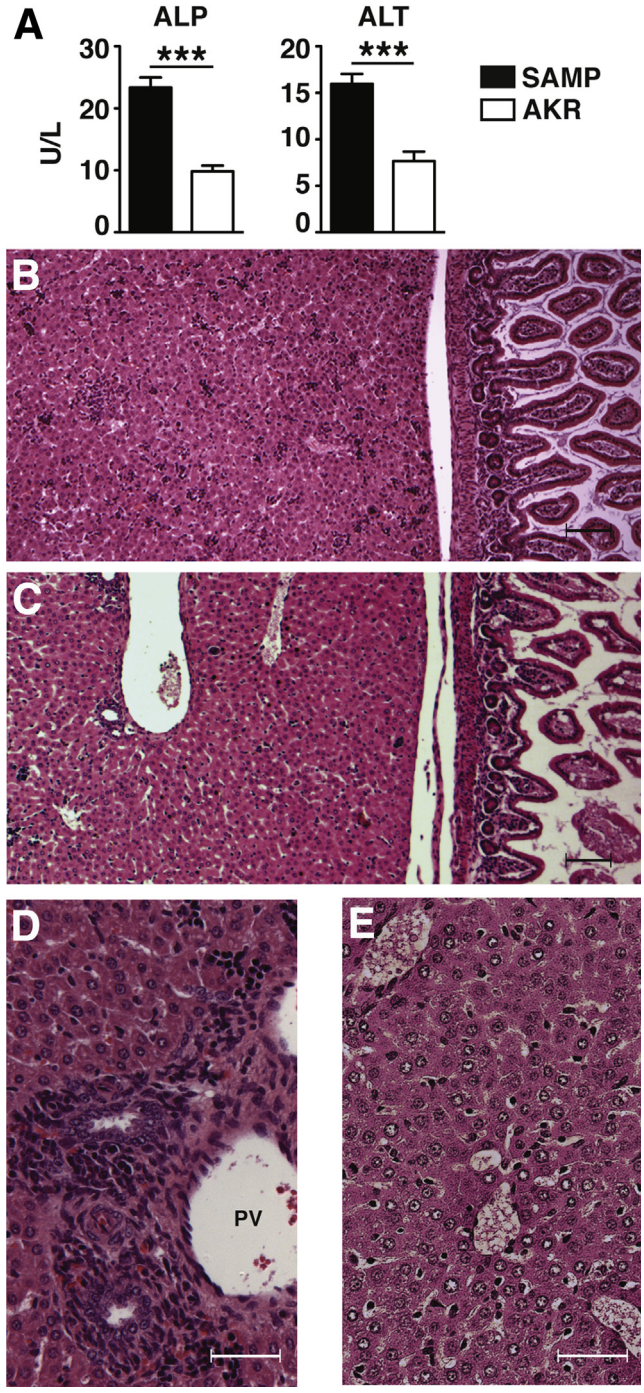

Figure 1. Liver inflammation in young, ileitis-prone SAMP1/YitFc (SAMP). (*A*) Serum liver enzyme levels in 4-week-old mice (n = 12). Representative histologic photomicrographs of (*B, D*) inflamed neonatal (1-week-old) SAMP liver with enlarged portal tracts filled with dense inflammatory infiltrates surrounding bile ducts versus (*C, E*) age-matched AKR/J (AKR) with normal, noninflamed morphology. PV, portal vein. Bars: (*B, C*) 100 μm, (*D, E*) 20 μm; ***$P < .001$.

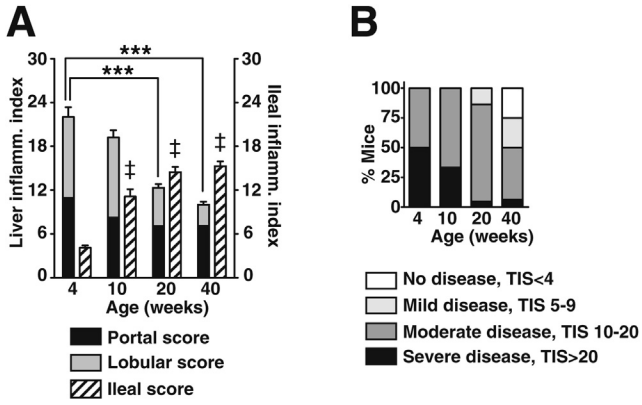

Figure 2. Liver inflammation in SAMP1/YitFc (SAMP) precedes ileitis and decreases over time. (*A*) Time-course of SAMP liver and ileal inflammation (n = 24). (*B*) Incidence and severity of liver disease (n = 24). TIS = total inflammatory score. $^{***}P < .001$, $^{‡}P < .01$ versus 4-week-olds.

either the onset or severity of liver inflammation (data not shown).

The main histopathologic features in SAMP livers consisted of portal tract inflammation characterized by lymphocytic infiltrates, eosinophilic polymorphonuclear cells, macrophages, as well as focal hepatitis with lymphocytes infiltrating the portal-parenchymal interface (Figure 4*A*) with inflammatory bridging between portal tracts (see Figure 4*B*). In addition to prominent portal tract involvement, other pathologic features recapitulated most of those described in IBD,[1] such as hepatocyte anisokaryosis, granuloma-like organization of lobular inflammatory infiltrates, and sinusoidal inflammation with mild microvesicular steatosis (see Figure 4*D–F*). Remarkably, the bile duct epithelium displayed evident ductular proliferation (see Figure 4*C*) and was focally infiltrated by $CD3^+$ T lymphocytes (see Figure 4*G*). Overall, the general histopathologic findings were indicative of immune-mediated liver disease involving both portal tracts and liver lobules with infiltration of biliary ducts, reminiscent of the clinical phenotype of PSC/AIH overlap syndrome.

Lymphocytes Are Required to Induce Liver Inflammation in SAMP and Consist Predominantly of Activated $CD4^+$ T Cells

We further characterized the immune cell infiltrates in young SAMP liver during the peak of inflammation by flow cytometry accordingly to the gating strategy illustrated in Figure 5. A marked increase in $CD3^+$ T-lymphocytes previously highlighted by immunohistochemistry (see Figure 4*G*) was confirmed in SAMP compared with AKR livers (Figure 6*A* and *B*). Surprisingly, the frequencies of hepatic $F4/80^+$ macrophages, $CD11c^+$ DCs, and $CD19^+$ B-lymphocytes, comparing the SAMP and AKR mice, were not significantly different for either cell percentages or absolute cell numbers (see Figure 6*A* and *B*). In addition, the cytokine mRNA expression measured in 4-week-old SAMP livers showed increased interleukin 1β (IL-1β), interferon-γ (IFNγ), and tumor necrosis factor, and decreased IL-4, IL-13, and IL-10 compared with age-matched AKR mice (see Figure 6*C*), demonstrating

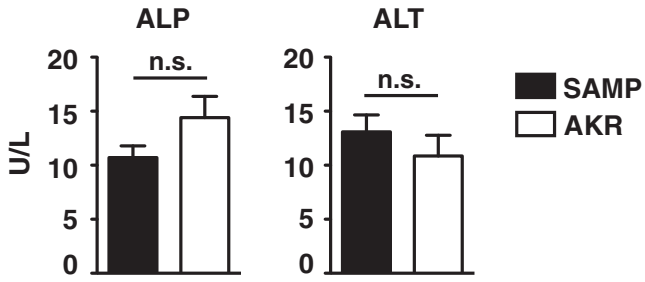

Figure 3. Circulating levels of alkaline phosphatase (ALP) and alanine aminotransferase (ALT) are comparable in SAMP1/YitFc (SAMP) versus AKR/J (AKR) mice at 20 weeks of age. Serum liver enzyme levels in 20-week-old mice as measured by enzyme-linked immunosorbent assay (n = 12). n.s., not statistically significant.

that the cytokine milieu during peak hepatic inflammation is skewed toward a proinflammatory/T_H1 profile.

Based on these data, we evaluated the requirement of lymphocytes for the development of SAMP hepatic inflammation. As such, we generated SAMPX*Rag-1*$^{-/-}$ mice by backcrossing *Rag-1*-deficient mice[24] onto the SAMP background to produce SAMP lacking mature T and B lymphocytes. We found that SAMPX*Rag-1*$^{-/-}$ mice developed only mild, if any, liver inflammation compared with SAMPX*Rag-1*$^{+/+}$ littermates (Figure 7*A*). Similarly, SAMPX*Rag-1*$^{-/-}$ mice also displayed attenuated ileitis compared with SAMPX*Rag-1*$^{+/+}$ littermates at 10 and 20 weeks (see Figure 7*B*) when ileal inflammation is normally established in native SAMP mice, whereas similar levels of inflammation were observed at 4 weeks of age.

Given the abundance of T lymphocytes in SAMP livers and their suggested role in IBD-associated liver diseases,[25] we measured the frequency of $CD4^+$ and $CD8^+$ subsets in 4-week-old SAMP and AKR livers. Interestingly, $CD4^+$ but not $CD8^+$ T cells were increased in SAMP livers and displayed a greater expression of the activation markers CD69 and CD44 compared with $CD4^+$ T-cells from AKR livers (see Figure 7*C*). The activated phenotype of SAMP intrahepatic $CD4^+$ T cells was consistent with the increased production of proinflammatory/T_H1 cytokines by NPLC (see Figure 6*C*). These data suggest the presence of an increased pool of activated intrahepatic $CD4^+$ Teff population in SAMP liver, which may play a role in the liver inflammation.

SAMP-Derived Hepatic $CD4^+$ T Cells Can Transfer Both Liver Inflammation and Ileitis Into Immunodeficient Recipient Mice Whereas Gut-Associated Lymphoid Tissue-Derived $CD4^+$ T Cells Transfer Only Ileitis

Given the ability of gut-associated lymphoid tissue (GALT)-derived $CD4^+$ T cells from SAMP mice to induce ileitis when adoptively transferred into immunodeficient recipients,[11,17,19,26] we tested the in vivo pathogenic potential of SAMP intrahepatic $CD4^+$ T cells. The $CD4^+$ T cells were isolated from MLNs and livers of 10- to 12-week-old SAMP and AKR mice (an age when both liver and ileal inflammation

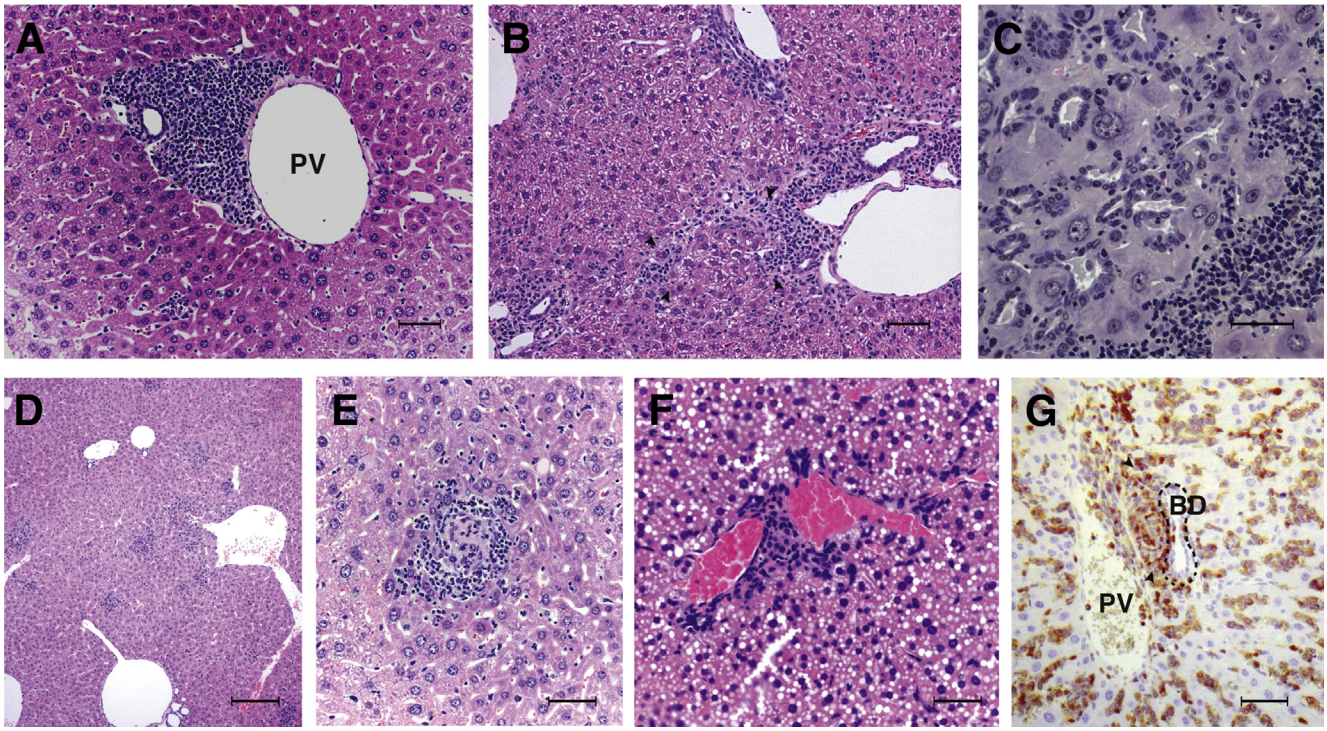

Figure 4. Histologic features of SAMP1/YitFc (SAMP) hepatic inflammation closely resemble liver disease observed in inflammatory bowel disease (IBD) patients. Main, pathologic features of SAMP liver include (*A*) infiltration of the portal-parenchymal interface with (*B*) occasional inflammatory bridging (*arrows*) between portal tracts, (*C*) ductular proliferation, and (*D*) hepatocyte anisokaryosis with inflammatory infiltration of liver lobules, often in the form of (*E*) granulomas. In a limited number of SAMP, (*F*) mild microvesicular steatosis occurs in association with sinusoidal inflammation. Importantly, (*G*) focal $CD3^+$ T-cell infiltration (*arrows*) was observed in the bile duct epithelium. BD, bile duct; PV, portal vein. Bars: (*A–C, E*) 50 μm, (*F, G*) 20 μm, and (*D*) 100 μm.

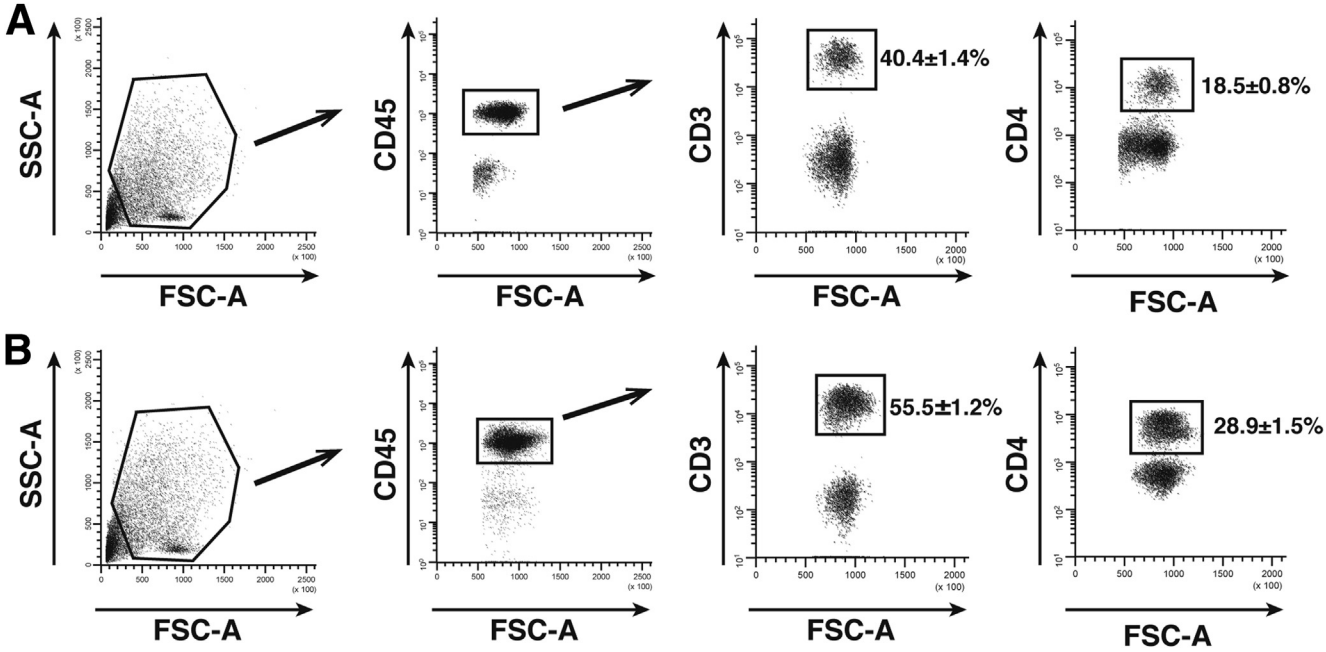

Figure 5. Flow cytometric strategy for analysis of hematopoietic cells in SAMP1/YitFc (SAMP) and AKR/J (AKR) livers. Nonparenchymal liver cells (NPLC) were isolated from (*A*) AKR and (*B*) SAMP livers by enzymatic digestion and used for flow cytometric analysis without any additional enrichment. Figure shows sequential gating on nondebris cells by FSC-A and SSC-A, followed by exclusion of nonhematopoietic cells by CD45 positive expression. $CD45^+$ hematopoietic cells were then investigated for additional markers. Representative plots for CD3 and CD4 expression in (*A*) AKR and (*B*) SAMP livers are shown.

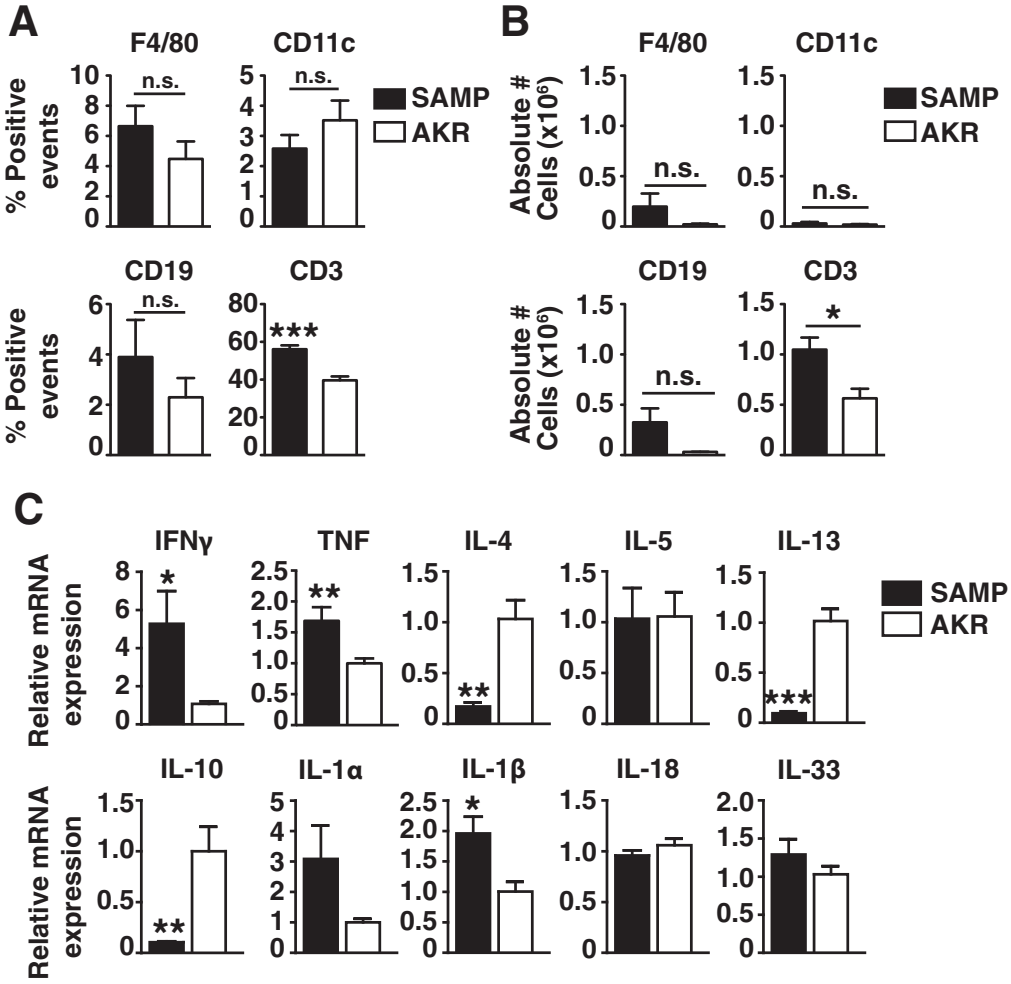

Figure 6. SAMP1/YitFc (SAMP) liver is abundantly infiltrated with T lymphocytes that display a T_H1-skewed cytokine profile. (*A*) Percentages and (*B*) absolute numbers (Abs #) of intrahepatic positive cells for F4/80, CD11c, CD19, and CD3 in total cell gate from young SAMP and AKR/J (AKR); one observation (n) represents pooled samples from two mice (n = 4). (*C*) Relative mRNA expression of hepatic T_H1, T_H2, and proinflammatory cytokines in nonparenchymal liver cells (NPLC) from 4-week-old mice (n = 8). $^*P < .05$, $^{**}P < .01$, $^{***}P < .001$ versus AKR. n.s., not statistically significant.

are established) and adoptively transferred into SCID mice. Our results showed that naïve SCIDs receiving $CD4^+$ T cells from SAMP livers progressively lost more body weight compared with those receiving cells from SAMP MLNs whereas SCIDs receiving no cells (control) or donor $CD4^+$ T cells from AKR mice increasingly gained weight (Figure 8*A*). Liver inflammation developed after adoptive transfer of liver-derived $CD4^+$ T cells from SAMP whereas MLN-derived cells

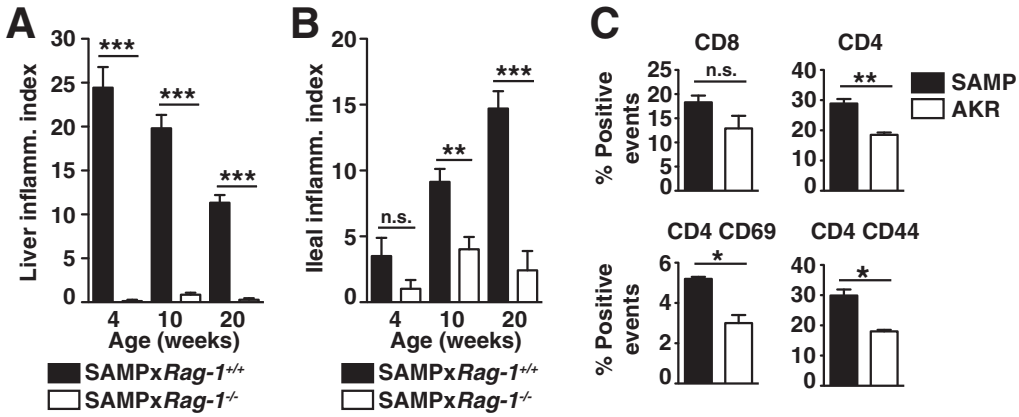

Figure 7. Lymphocytes are required to induce hepatic inflammation and display an activated phenotype in SAMP1/YitFc (SAMP) livers. Severity of (*A*) liver and (*B*) ileal inflammation in SAMPX*Rag-1*$^{-/-}$ versus SAMPX*Rag-1*$^{+/+}$ mice (n = 7). (*C*) Percentages of intrahepatic positive cells for CD8 and CD4 within the total cell population, as well as CD69 and CD44 within the CD4 positive gate from 4-week-old SAMP and AKR/J (AKR) (n = 8); $^*P < .05$, $^{**}P < .01$, $^{***}P < .001$ versus AKR or SAMPx*Rag-1*$^{+/+}$. n.s., not statistically significant.

were not able to induce significant liver inflammation versus AKR donor T cells (see Figure 8*B*).

Importantly, the prominent ileitis that developed in recipient mice after transfer of liver-derived SAMP CD4$^+$ T cells was more severe than the ileitis observed after transfer of MLN-derived cells as well as in the control (untransferred) recipients, which displayed no histologic signs of inflammation (see Figure 8*B* and *C*). Similar to

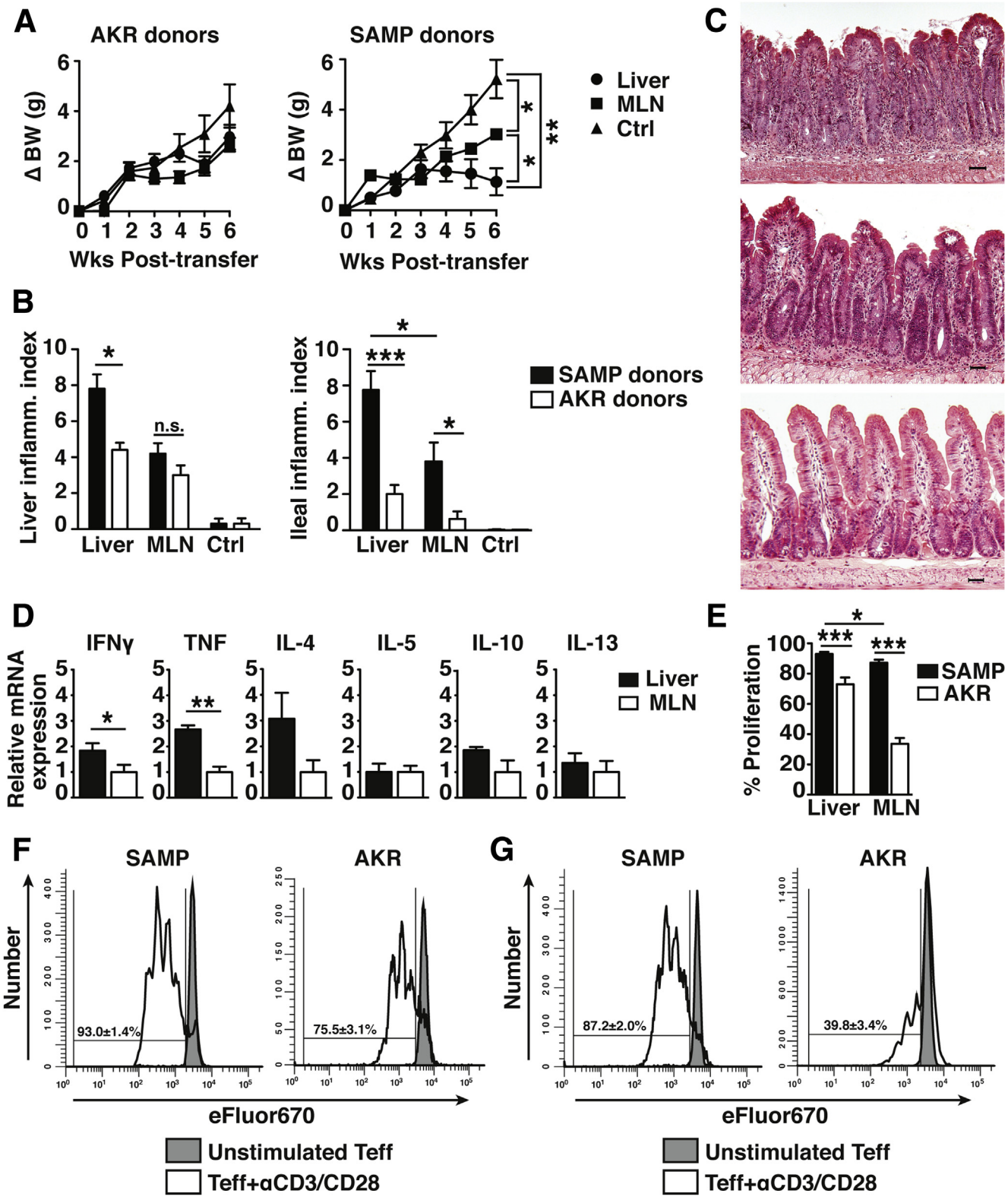

native SAMP (see Figure 6*C*), intrahepatic $CD4^+$ T cells from SCIDs receiving SAMP liver cells expressed higher mRNA transcript levels of tumor necrosis factor and IFNγ compared with those receiving MLN T cells (see Figure 8*D*).

We next asked whether the activated phenotype of SAMP hepatic $CD4^+$ T cells results in greater proliferation of $CD4^+$ Teff cells, which may explain the increased severity of ileitis induced in SCID recipients receiving liver-derived compared with MLN-derived $CD4^+$ T cells. Interestingly, the percentage of dividing cells was significantly increased (reduced 5-(6)-carboxyfluorescein diacetate succinimidyl ester) in 10-week-old SAMP livers compared with AKR livers. Although both SAMP liver- and MLN-derived Teff displayed increased percentages of proliferating cells compared with AKR controls, the liver-derived Teff showed greater proliferation than MLN-derived Teff from SAMP mice (see Figure 8*E*–*G*). A greater proliferation of Teff was observed in both SAMP and AKR liver-versus MLN-derived cells, suggesting increased activation of the liver compared to GALT, although only SAMP intrahepatic $CD4^+$ T cells are able to induce liver inflammation in SCID recipients. Together, these data suggest that the heightened activation status of SAMP hepatic Teff cells may partially account for the increased pathogenic potential of these cells compared to GALT- and liver-derived AKR Teff cells.

Accumulation of $\alpha_4\beta_7^+$ $CCR9^+$ $CD4^+$ T Cells Is Not Present in Inflamed SAMP Versus AKR Livers

According to the most commonly accepted hypothesis, IBD-associated liver inflammation is the result of lymphocyte homing, specifically of either $\alpha_4\beta_7^+$ and/or $CCR9^+$ cells that are originally activated in the gut and subsequently recruited to the liver.[2] Therefore, we asked whether accumulation of either $\alpha_4\beta_7^+$ and/or $CCR9^+$ $CD4^+$ T lymphocytes could be observed during established hepatic inflammation in SAMP, similarly to what is observed for $CD8^+$ T lymphocytes in PSC patients.[4,5] Interestingly, no differences in the percentages of $CD4^+$ T cells positive or highly expressing $\alpha_4\beta_7$ and/or CCR9 were observed in SAMP versus AKR livers (Figure 9*A*). However, when absolute numbers of $\alpha_4\beta_7^+$ and $CCR9^+$ $CD4^+$ T cells were measured, we observed an increase in $\alpha_4\beta_7^+$, $\alpha_4\beta_7^{high}$, and $CCR9^+$ $CD4^+$ T cells (see Figure 9B), which likely reflects the increased cellularity of SAMP versus AKR livers (see Figure 9*C*).

To clarify whether increased expression of $\alpha_4\beta_7$ and CCR9 within intrahepatic $CD4^+$ T cells results from the recruitment of gut-activated $\alpha_4\beta_7^+$ and $CCR9^+$ $CD4^+$ T lymphocytes or, alternatively, from local imprinting of these molecules,[27] we evaluated protein expression of MAdCAM-1 and CCL25, the cognate ligands for $\alpha_4\beta_7$ and CCR9, respectively, for which aberrant hepatic expression is thought to facilitate recruitment of gut-activated T-lymphocytes to the liver in PSC.[4,5] MAdCAM-1 and CCL25 protein expression, however, was unchanged in SAMP compared with AKR livers (see Figure 9*D*), suggesting that the expression of $\alpha_4\beta_7^+$ and $CCR9^+$ is likely imprinted to $CD4^+$ T cells in the SAMP liver. In fact, differently from other hepatic APCs, LSEC have been reported to promote gut tropism by inducing expression of $\alpha4\beta7$ and CCR9 on $CD4^+$ T cells within the liver.[27] Although LSEC frequency is decreased in the SAMP versus AKR liver (Figure 10*A*), these cells display an increase in MHC class II expression compared to those found in AKR livers (see Figure 10*B*), suggesting increased antigen presentation to $CD4^+$ T cells in SAMP versus AKR livers. Together, these data suggest that enhanced recruitment of gut-activated $CD4^+$ T cells to the liver is not likely the main initiating factor driving liver inflammation in SAMP mice.

SAMP Liver-Derived Regulatory T Cells Are Impaired in Their In Vitro Immunosuppressive Capability

Because it is unlikely that the bulk of activated intrahepatic $CD4^+$ T cells are recruited from the gut to initiate SAMP liver inflammation, we asked whether locally impaired immunosuppression may occur within the liver of these mice. First, we measured the frequency of $FoxP3^+$ Tregs within the $CD4^+$ gate by flow cytometry in SAMP and AKR livers. Although the percentages of Tregs were decreased within the overall $CD4^+$ population (Figure 11*A* and *B*), there was no significant difference in the absolute numbers of Tregs in SAMP compared with AKR livers (see Figure 11*C*), which again, is likely due to the increased cellularity observed in SAMP livers (see Figure 9*C*). These data suggest that Tregs are likely outnumbered within the

Figure 8. (*See previous page*). SAMP1/YitFc (SAMP) intrahepatic T_H1 effector T cells (Teff) transfer both liver inflammation and ileitis. (*A*) Change in body weight (ΔBW), and (*B*) liver and ileal inflammation in recipient mice after adoptive transfer of donor $CD4^+$ T cells; recipients receiving vehicle only served as controls (Ctrl) (n = 8). (*C*) Representative histologic photomicrographs displaying epithelial crypt hypertrophy and elongation, and villous blunting with dense inflammatory infiltrates throughout mucosa and submucosa in recipients of liver-derived donor cells (*top*), which were less severe in ilea adoptively transferred with mesenteric lymph node (MLN)-derived donor cells (*middle*) and Ctrl (*lower*). (*D*) T_H1/T_H2 cytokine mRNA expression in activated ex vivo cultured intrahepatic $CD4^+$ T cells from recipients of donor SAMP liver versus MLN cells. (*E*) Percentages of Teff proliferation in liver and MLN of 10-week-old SAMP and AKR/J (AKR) mice. Percentages represent dividing cells in the presence of αCD3/CD28. Results are from four independent experiments (five mice pooled per experiment). (*F, G*) Representative histograms show proliferation of (*F*) liver- and (*G*) MLN-derived viable, CD4-gated cells in the absence (*gray peaks*) and presence (*white peaks*) of αCD3/CD28. Percentages represent dividing cells in the presence of αCD3/CD28. Bars: 50μm; $^*P < .05$, $^{**}P < .01$, $^{***}P < .005$ versus SCID receiving AKR donor cells, SAMP MLN-derived donor cells or AKR controls. n.s., not statistically significant.

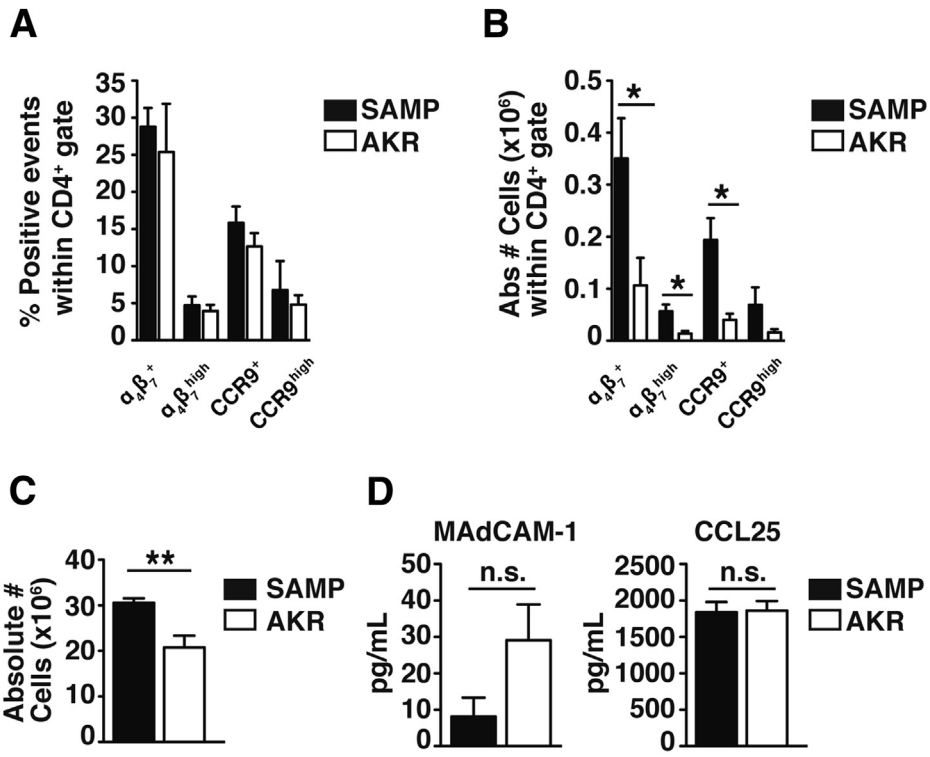

Figure 9. In SAMP1/YitFc (SAMP) livers, $\alpha_4\beta_7^+$ and CCR9$^+$ CD4$^+$ T cells do not accumulate. (*A*) Percentages and (*B*) absolute numbers (Abs #) of intrahepatic CD4$^+$ T-cell subsets from 4-week-old SAMP and AKR/J (AKR). Isolated nonparenchymal liver cells (NPLC) were first gated on CD4 and successively on $\alpha_4\beta_7$ and CCR9, distinguishing between overall positive cells and highly expressing cells; one observation (n) represents pooled samples from two mice (n = 5). (*C*) Total NPLC numbers (#) isolated by enzymatic digestion without any additional enrichment from 10-week-old SAMP and AKR livers (n = 8). (*D*) Protein concentrations of hepatic mucosal addressin cell adhesion molecule-1 (MAdCAM-1) and CC chemokine ligand 25 (CCL25) (n = 6). n.s. = not statistically significant.

CD4$^+$ compartment by proliferating Teff cells rather than decreased in absolute number in SAMP versus AKR livers.

In addition, to test whether the immunosuppressive function of liver-resident Tregs is altered in SAMP, we evaluated the capacity of Tregs to suppress in vitro proliferation of Teff cells. Teff (CD4$^+$CD25$^-$) and Treg (CD4$^+$CD25$^+$) cells were isolated from SAMP and AKR livers by FACS, accordingly to the strategy depicted in Figure 12. Suppression by Tregs is expressed as the percentage of proliferating cells (eFluor 670 "low") inhibited after coculture with Tregs, and was calculated by normalizing the difference of proliferating cells with Tregs to the proliferation in the absence of Tregs. Interestingly, liver-resident Tregs from SAMP were less effective at suppressing the proliferation of hepatic Teff cells compared with Tregs from AKR (see Figure 11*D* and *E*).

These data demonstrate that liver-resident Tregs from SAMP are dysfunctional in vitro and unable to suppress the proliferation of hepatic Teff cells as effectively as Tregs from AKR control mice. Overall, these findings suggest that impaired suppressive function of hepatic Tregs in SAMP liver is permission for the unrestrained proliferation of pathogenic T_H1-activated CD4$^+$ T cells, resulting in a biased, increased Teff/Treg ratio that leads to liver inflammation in these mice.

Discussion

Although liver disease has previously been reported in ileitis-prone SAMP mice,[13,14] the precise histologic features, onset and progression of disease, pathogenic mechanism(s), and it's the translational implications to IBD have not been fully addressed. Interestingly, evaluation of SAMP livers suggests a clinical phenotype resembling PSC/AIH overlap syndrome, which can also represent a comorbidity with IBD[1]. PSC/AIH overlap syndrome is defined as an immune-mediated disorder with cholangiographic findings, and histologic, biologic and/or clinical features of AIH. Histologic characteristics of AIH include piecemeal necrosis, lymphocyte rosetting, and moderate to severe periportal or periseptal inflammation,[28] which are features also found in SAMP livers (see Figure 1*B* and *D*, and Figure 4). Nonetheless, although SAMP mice exhibit many histologic

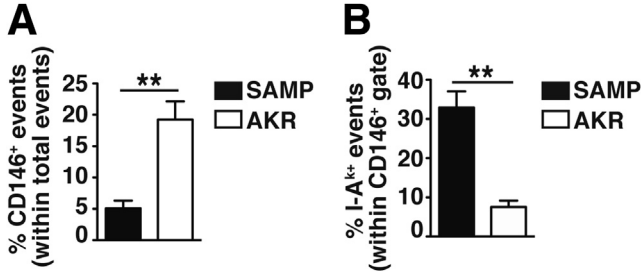

Figure 10. Liver sinusoidal endothelial cells (LSEC) are decreased in SAMP1/YitFc (SAMP) livers but display greater expression of MHC class II compared with AKR/J (AKR) livers. (*A*) Percentages of intrahepatic positive cells for CD146$^+$ (LSEC) in total cell gate, and for (*B*) IA^k in CD146$^+$ gate in inflamed young SAMP and AKR controls. One observation (n) represents pooled samples from two mice (n = 5).

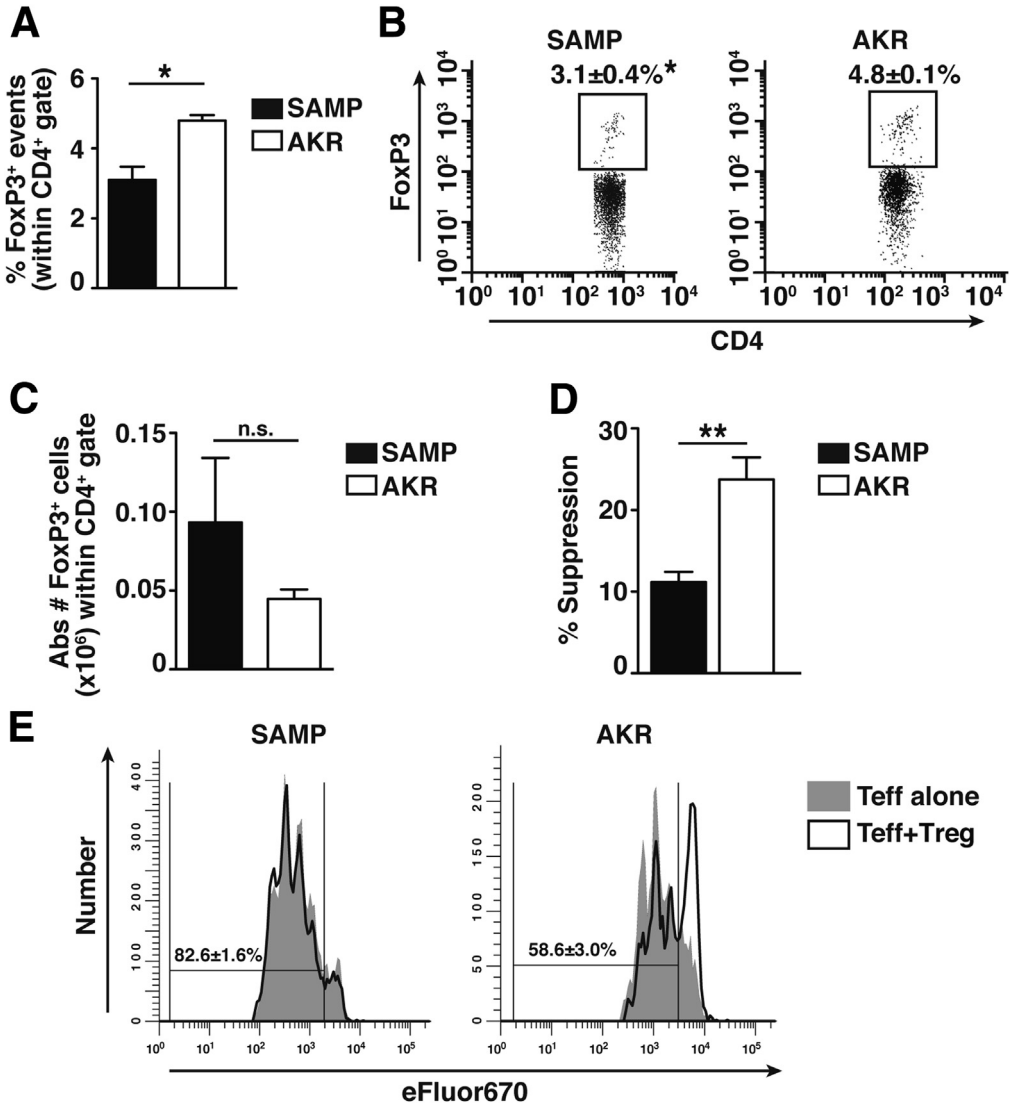

Figure 11. In vitro suppressive function of regulatory T cells (Tregs) but not their absolute number is altered in SAMP1/YitFc (SAMP) versus AKR/J (AKR) livers. (*A*) Percentages of intrahepatic FoxP3$^+$ cells calculated within CD4$^+$ gate, with (*B*) representative plots (n = 3) in young SAMP and AKR. (*C*) Absolutes number (Abs #) of intrahepatic FoxP3$^+$ cells isolated per mouse were calculated within CD4$^+$ gate. (*D*) In vitro Treg suppression activity in livers of young SAMP and AKR mice. Percent suppression is expressed as the percentage of effector T cell (Teff) proliferation that was suppressed by coculture with Tregs. Results are from four independent experiments (15 mice pooled per experiment). (*E*) Representative histograms showing proliferation of viable, CD4-gated cells in the absence (gray peaks) and presence (white peaks) of hepatic Tregs. Percentages represent dividing cells in the presence of Tregs. *$P < .05$, **$P < .001$. n.s., not statistically significant.

similarities to PSC patients, SAMP hepatic inflammation does not fully represent classic PSC but rather a comorbidity model of IBD and inflammatory liver disease. In fact, PSC-associated IBD also displays different clinical manifestations with respect to IBD alone, suggesting that PSC-associated IBD may constitute a unique IBD phenotype in itself.[29]

As such, SAMP mice may serve as an informative and useful model for PSC, but also other types of inflammatory liver diseases that coexist with IBD. Importantly, although liver involvement in IBD is commonly regarded as a consequential secondary event to gut inflammation, we report peak hepatic inflammation in SAMP at 4 weeks of age, before the onset of ileitis (see Figure 2*A*). This finding suggests that in SAMP the presence of an inflamed gut is not required to trigger hepatic inflammation and that other mechanism(s) intrinsic to the liver or host may induce liver disease.

The absence of hepatic inflammation observed in SAMPX*Rag-1*$^{-/-}$ mice (see Figure 7*A*), wherein the lack of mature lymphocytes is sufficient to abrogate liver disease, demonstrates that functional lymphocytes are required for the development of SAMP liver disease. Moreover, in the absence of mature lymphocytes, the amelioration of disease was more pronounced in the liver than in the ileum when comparing the relative reduction in inflammatory scores from SAMPX*Rag-1*$^{-/-}$ versus SAMPX*Rag-1*$^{+/+}$ control mice (see Figure 7*A* and *B*). As such, although lymphocytes appear to play a pivotal role in SAMP ileitis,[12] the contribution of the nonhematopoietic compartment[16] appears to be particularly crucial for ileal, compared to liver, inflammation to develop.

Furthermore, the abundant accumulation of T but not B lymphocytes in the inflammatory infiltrates of SAMP liver (see Figure 6*A* and *B*) suggests that these cells may play a role in inducing and/or sustaining the hepatic inflammation in SAMP mice. Similar to the early inductive phase of ileitis wherein T_H1 cytokines predominate,[11] the SAMP hepatic environment is also T_H1-biased (see Figure 6*C*) and enriched for activated CD4$^+$ T cells (see

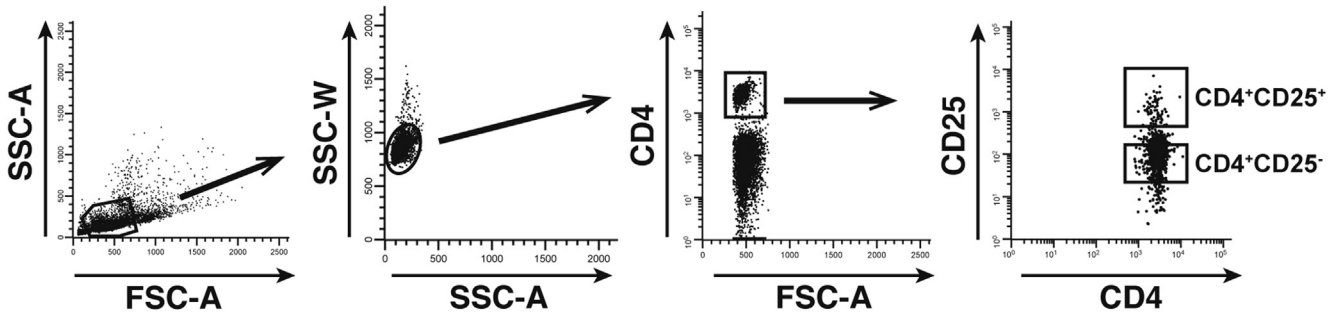

Figure 12. FACS sorting strategy for isolation of $CD4^+CD25^-$ and $CD4^+CD25^+$ cells. $CD4^+CD25^-$ and $CD4^+CD25^+$ cells were isolated from SAMP1/YitFc (SAMP) and AKR/J (AKR) mice, using Percoll gradients for livers and CD4 magnetic beads for mesenteric lymph node cells (MLNs), followed by FACS. Figure shows sequential gating on lymphocytes by FSC-A and SSC-A, followed by exclusion of aggregates by SSC-W and SSC-A. Singlet lymphocytes were selected on CD4 positive fluorescence and then on CD25 positive regulatory T (Treg) or negative effector T (Teff) expression.

Figure 7*C*). This T_H1 milieu is already established by 4 weeks, before ileitis, which suggests the presence of a shared $CD4^+$ T-cell-mediated pathogenic mechanism between the two organs that is able to induce similar phenotypes and immune responses, albeit temporally separated. Moreover, SAMP-derived intrahepatic $CD4^+$ T cells are able to adoptively transfer both liver and ileal inflammation, whereas GALT-derived $CD4^+$ T cells induce milder ileitis with respect to liver-derived cells but are not sufficient to transfer liver inflammation (see Figure 8*B*).

Interestingly, the increased activation status of Teff observed in SAMP liver (see Figure 8*E*) could partially account for the increased pathogenic potential of these cells and their ability to induce liver inflammation in SCID recipients. Although the greater proliferation observed in AKR liver- versus MLN-derived Teff cells suggests an increased baseline activation of the liver compared with GALT, only SAMP intrahepatic $CD4^+$ T cells are able to induce liver inflammation in SCID recipients. Therefore, the unique pathogenic potential of SAMP intrahepatic $CD4^+$ T cells appears to be both organ- and host-restricted. These results suggest that the liver, rather than the gut, may provide a pool of pathogenic T_H1 $CD4^+$ T cells able to induce hepatic inflammation, contrary to the widely accepted hypothesis that IBD-associated liver inflammation is mediated by long-lived, GALT-derived $\alpha4\beta7^+$ and $CCR9^+$ T-lymphocytes later recruited to the liver.[5,25,30] In addition, although the absolute numbers of intrahepatic $\alpha4\beta7^+$ and $CCR9^+$ $CD4^+$ T cells were increased in SAMP versus AKR livers (see Figure 9*B*), we were unable to detect any significant differences in either the percentages of intrahepatic $\alpha4\beta7^+$ and $CCR9^+$ $CD4^+$ T cells or their corresponding ligands MAdCAM-1 and CCL25 during peak hepatic inflammation in SAMP versus AKR (see Figure 9*A* and *D*), which is different from what has been observed for the ileal phenotype.[14,20,21,31] This provides further evidence supporting the hypothesis that host hepatic defects rather than aberrant recruitment of gut-activated lymphocytes may be responsible for the ileitis-associated liver phenotype observed in SAMP mice.

Effector functions of intrahepatic T-lymphocytes depend both on their site of primary activation and on the type of T cells considered, particularly whether these are $CD4^+$ or $CD8^+$ T lymphocytes.[6,32] Increasing evidence suggests that antigen presentation in the liver mainly results in activation of $CD8^+$ T cells whereas the effect on $CD4^+$ lymphocytes is still controversial.[7,8,33] Despite the proinflammatory environment characteristic of the SAMP liver during peak inflammation, we could not detect significant differences in intrahepatic DC and macrophage (KC) frequencies (see Figure 6*A* and *B*) and their MHC class II expression (Figure 13*A* and *B*) when comparing the SAMP and AKR livers. Therefore, increased antigen presentation by traditional liver-resident APCs are unlikely to represent the main mechanism by which $CD4^+$ T cells acquire pathogenic potential in the inflamed SAMP liver.

The hypothesis that unrestrained proliferation of Teff cells contributes to IBD-associated liver disease has already been suggested by the ability of $CD4^+CD45RB^{high}$ cells to induce liver inflammation together with colon and small bowel inflammation when transferred into lymphopenic mice.[34] Nevertheless, the role of Teff cells versus regulatory compartments has not been thoroughly investigated in IBD-associated liver disease. We report a diminished percentage of SAMP hepatic $FoxP3^+$ Tregs in the overall $CD4^+$ compartment; however, the absolute numbers are unchanged with respect to AKR livers (see Figure 11*A*–*C*), suggesting that the homeostatic Teff/Treg ratio is altered in the inflamed SAMP

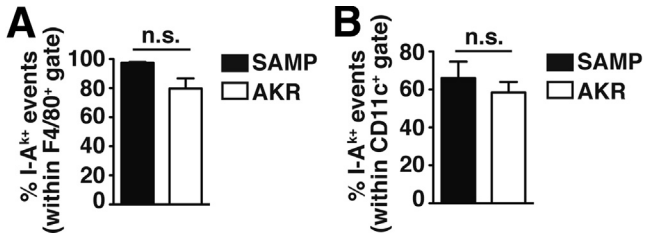

Figure 13. MHC class II expression is not increased in SAMP1/YitFc (SAMP) versus AKR/J (AKR) hepatic dendritic cells (DC) and Kupffer cells (KC). Percentages of intrahepatic positive cells for IA^k within (*A*) $F4/80^+$ gate (KC) and (*B*) $CD11c^+$ gate (DC) in inflamed young SAMP and AKR controls. One observation (n) represents pooled samples from two mice (n = 5).

liver. Moreover, in vitro evaluation of the Treg suppressive capacity indicates that SAMP hepatic Tregs are dysfunctional, similar to what has been observed for SAMP ileitis.[35]

Mechanistically, the disruption of hepatic tolerance in favor of uncontrolled proliferation of pathogenic T_H1 $CD4^+$ T cells may also be facilitated by altered LSEC frequency and function. Indeed, LSEC can induce both FoxP3 positive and negative Tregs, but they can also suppress CD4 and CD8 effector T cells[8,36–38] and are considered to be critical for promoting hepatic T-cell tolerance. Typically, antigen presentation by LSEC to $CD4^+$ T cells does not result in an effective immune response but rather leads to the induction of hepatic tolerance.[8,33] LSEC normally express low levels of MHC class II as a consequence of exposure to IL-10, abundant in the homeostatic liver, which determines a shift from an activated to inhibitory phenotype with the ability to suppress IFNγ secretion from $CD4^+$ T cells.[36,39] $CD146^+$ LSEC are not only decreased in frequency in inflamed SAMP livers but also display a greater expression of MHC class II (see Figure 10), consistent with increased expression of $\alpha4\beta7$ and CCR9 among intrahepatic $CD4^+$ T cells (see Figure 9*A*), as well as diminished IL-10 in SAMP NPLC (see Figure 6*C*). As such, down-regulation of IL-10 in inflamed SAMP livers could determine a shift in LSEC phenotype and function, impairing their ability to effectively suppress T_H1 $CD4^+$ T cells.

Overall, these results support a pathogenic role for inherent intrahepatic $CD4^+$ T cells in SAMP liver and intestinal inflammation, and suggest that impaired hepatic immune tolerance may be responsible for their acquired pathogenicity and function. These findings also raise the possibility that IBD-associated liver disease does not simply represent an extraintestinal manifestation of a primary inflammatory gut phenotype, but that liver and intestinal inflammation in IBD patients may develop as concomitant disease processes based on common host-driven immune defects.

References

1. Navaneethan U, Shen B. Hepatopancreatobiliary manifestations and complications associated with inflammatory bowel disease. Inflamm Bowel Dis 2010;16:1598–1619.
2. Adams DH, Eksteen B, Curbishley SM. Immunology of the gut and liver: a love/hate relationship. Gut 2008; 57:838–848.
3. Tufail S, Badrealam KF, Sherwani A, et al. Tissue specific heterogeneity in effector immune cell response. Front Immunol 2013;4:254.
4. Grant AJ, Lalor PF, Hubscher SG, et al. MAdCAM-1 expressed in chronic inflammatory liver disease supports mucosal lymphocyte adhesion to hepatic endothelium (MAdCAM-1 in chronic inflammatory liver disease). Hepatology 2001;33:1065–1072.
5. Eksteen B, Grant AJ, Miles A, et al. Hepatic endothelial CCL25 mediates the recruitment of $CCR9^+$ gut-homing lymphocytes to the liver in primary sclerosing cholangitis. J Exp Med 2004;200:1511–1517.
6. Derkow K, Loddenkemper C, Mintern J, et al. Differential priming of CD8 and CD4 T-cells in animal models of autoimmune hepatitis and cholangitis. Hepatology 2007; 46:1155–1165.
7. Bertolino P, Bowen DG, McCaughan GW, et al. Antigen-specific primary activation of $CD8^+$ T cells within the liver. J Immunol 2001;166:5430–5438.
8. Kruse N, Neumann K, Schrage A, et al. Priming of $CD4^+$ T cells by liver sinusoidal endothelial cells induces $CD25^{low}$ forkhead box protein 3^- regulatory T cells suppressing autoimmune hepatitis. Hepatology 2009; 50:1904–1913.
9. Thomson AW, Knolle PA. Antigen-presenting cell function in the tolerogenic liver environment. Nat Rev Immunol 2010;10:753–766.
10. Racanelli V, Rehermann B. The liver as an immunological organ. Hepatology 2006;43:S54–S62.
11. Kosiewicz MM, Nast CC, Krishnan A, et al. Th1-type responses mediate spontaneous ileitis in a novel murine model of Crohn's disease. J Clin Invest 2001;107:695–702.
12. Pizarro TT, Pastorelli L, Bamias G, et al. SAMP1/YitFc mouse strain: a spontaneous model of Crohn's disease-like ileitis. Inflamm Bowel Dis 2011;17:2566–2584.
13. Matsumoto S, Okabe Y, Setoyama H, et al. Inflammatory bowel disease-like enteritis and caecitis in a senescence accelerated mouse P1/Yit strain. Gut 1998;43:71–78.
14. Rivera-Nieves J, Ho J, Bamias G, et al. Antibody blockade of CCL25/CCR9 ameliorates early but not late chronic murine ileitis. Gastroenterology 2006;131:1518–1529.
15. Reuter BK, Pastorelli L, Brogi M, et al. Spontaneous, immune-mediated gastric inflammation in SAMP1/YitFc mice, a model of Crohn's-like gastritis. Gastroenterology 2011;141:1709–1719.
16. Olson TS, Reuter BK, Scott KG, et al. The primary defect in experimental ileitis originates from a nonhematopoietic source. J Exp Med 2006;203:541–552.
17. Bamias G, Martin C, Mishina M, et al. Proinflammatory effects of T_H2 cytokines in a murine model of chronic small intestinal inflammation. Gastroenterology 2005; 128:654–666.
18. Bamias G, Okazawa A, Rivera-Nieves J, et al. Commensal bacteria exacerbate intestinal inflammation but are not essential for the development of murine ileitis. J Immunol 2007;178:1809–1818.
19. Olson TS, Bamias G, Naganuma M, et al. Expanded B cell population blocks regulatory T cells and exacerbates ileitis in a murine model of Crohn disease. J Clin Invest 2004;114:389–398.
20. Rivera-Nieves J, Olson T, Bamias G, et al. L-selectin, alpha 4 beta 1, and alpha 4 beta 7 integrins participate in $CD4^+$ T cell recruitment to chronically inflamed small intestine. J Immunol 2005;174:2343–2352.
21. Gorfu G, Rivera-Nieves J, Hoang S, et al. Beta7 integrin deficiency suppresses B cell homing and attenuates chronic ileitis in SAMP1/YitFc mice. J Immunol 2010; 185:5561–5568.
22. Pastorelli L, Garg RR, Hoang SB, et al. Epithelial-derived IL-33 and its receptor ST2 are dysregulated in ulcerative colitis and in experimental Th1/Th2 driven enteritis. Proc Natl Acad Sci USA 2010;107:8017–8022.
23. Goodman WA, Garg RR, Reuter BK, et al. Loss of estrogen-mediated immunoprotection underlies female gender bias in experimental Crohn's-like ileitis. Mucosal Immunol 2014;7:1255–1265.

24. Mombaerts P, Iacomini J, Johnson RS, et al. RAG-1-deficient mice have no mature B and T lymphocytes. Cell 1992;68:869–877.
25. Adams DH, Eksteen B. Aberrant homing of mucosal T cells and extra-intestinal manifestations of inflammatory bowel disease. Nat Rev Immunol 2006;6:244–251.
26. Takedatsu H, Mitsuyama K, Matsumoto S, et al. Interleukin-5 participates in the pathogenesis of ileitis in SAMP1/Yit mice. Eur J Immunol 2004;34:1561–1569.
27. Neumann K, Kruse N, Szilagyi B, et al. Connecting liver and gut: murine liver sinusoidal endothelium induces gut tropism of $CD4^+$ T cells via retinoic acid. Hepatology 2012;55:1976–1984.
28. Floreani A, Rizzotto ER, Ferrara F, et al. Clinical course and outcome of autoimmune hepatitis/primary sclerosing cholangitis overlap syndrome. Am J Gastroenterol 2005; 100:1516–1522.
29. Loftus EV Jr, Harewood GC, Loftus CG, et al. PSC-IBD: a unique form of inflammatory bowel disease associated with primary sclerosing cholangitis. Gut 2005; 54:91–96.
30. Eksteen B, Mora JR, Haughton EL, et al. Gut homing receptors on CD8 T cells are retinoic acid dependent and not maintained by liver dendritic or stellate cells. Gastroenterology 2009;137:320–329.
31. Matsuzaki K, Tsuzuki Y, Matsunaga H, et al. In vivo demonstration of T lymphocyte migration and amelioration of ileitis in intestinal mucosa of SAMP1/Yit mice by the inhibition of MAdCAM-1. Clin Exp Immunol 2005; 140:22–31.
32. Crispe IN. Immune tolerance in liver disease. Hepatology 2014;60:2109–2117.
33. Derkow K, Muller A, Eickmeier I, et al. Failure of CD4 T-cells to respond to liver-derived antigen and to provide help to CD8 T-cells. PLoS One 2011;6:e21847.
34. Ostanin DV, Bao J, Koboziev I, et al. T cell transfer model of chronic colitis: concepts, considerations, and tricks of the trade. Am J Physiol Gastrointest Liver Physiol 2009; 296:G135–G146.
35. Ishikawa D, Okazawa A, Corridoni D, et al. Tregs are dysfunctional in vivo in a spontaneous murine model of Crohn's disease. Mucosal Immunol 2013;6:267–275.
36. Carambia A, Frenzel C, Bruns OT, et al. Inhibition of inflammatory CD4 T cell activity by murine liver sinusoidal endothelial cells. J Hepatol 2013;58:112–118.
37. Carambia A, Freund B, Schwinge D, et al. TGF-beta-dependent induction of $CD4^+CD25^+Foxp3^+$ Tregs by liver sinusoidal endothelial cells. J Hepatol 2014;61:594–599.
38. Schildberg FA, Hegenbarth SI, Schumak B, et al. Liver sinusoidal endothelial cells veto CD8 T cell activation by antigen-presenting dendritic cells. Eur J Immunol 2008; 38:957–967.
39. Knolle PA, Uhrig A, Hegenbarth S, et al. IL-10 down-regulates T cell activation by antigen-presenting liver sinusoidal endothelial cells through decreased antigen uptake via the mannose receptor and lowered surface expression of accessory molecules. Clin Exp Immunol 1998;114:427–433.

Received April 2, 2015. Accepted May 23, 2015.

Correspondence
Address correspondence to: Theresa T. Pizarro, PhD, Department of Pathology, Case Western Reserve University School of Medicine, 2103 Cornell Road, WRB 5534, Cleveland, Ohio 44106. e-mail: theresa.pizarro@case.edu; fax: (216) 368-0494.

Acknowledgments
The authors thank Raffaella DeFranco, Brian Reuter, David DeSantis, Laura E. Nagy, Sharon Hoang, Xiao-Ming Wang, Danian Che, Hiram De Jesus, and Carlo De Salvo for their technical support and expertise, and James R. Mize for ileal histopathologic evaluation.

Conflicts of interest
The authors disclose no conflicts.

Funding
This study was funded by the National Institutes of Health, grants DK056762 and AI102269 (to T.T.P.) and DK042191, DK091222, and DK097948 (to F.C./T.T.P.).